Synthesis and Characterization of Polyphenols Derived from 4-Fluorobenzaldeyde: The Effect of Electron-Donating Group on Some Physical Properties

İsmet Kaya,[1] Musa Kamacı,[2] Fatih Arıcan[1]

[1]*Department of Chemistry, Faculty of Sciences and Arts, Çanakkale Onsekiz Mart University, 17020 Çanakkale, Turkey*
[2]*Department of Chemistry, Kamil Özdağ Science Faculty, Karamanoğlu Mehmetbey University, 70100 Karaman, Turkey*

Received 17 May 2011; accepted 23 September 2011
DOI 10.1002/app.36273
Published online 26 December 2011 in Wiley Online Library (wileyonlinelibrary.com).

ABSTRACT: In this study, we proposed to investigate how the effect of electron-donating methyl (—CH_3) group at *p*-position of amin (—NH_2) group in aminophenol (AP) compound affected thermal stability, optical, electrochemical properties, and conductivity measurement. For this reason, we choice 2-AP and 2-amino-4-methylphenol compounds and synthesized phenolic monomers by condensation reactions 4-fluorobenzaldehyde with aromatic amino phenols. Then, these monomers were converted to their polyphenol derivatives by oxidative polycondensation reactions in an aqueous alkaline medium. Structural characterizations were carried out by FTIR, NMR, and size exclusion chromatography. Cyclic voltammetry was used to determine the electrochemical oxidation-reduction characteristics. Optical properties were investigated by UV–vis and fluorescence analyses. Solid state electrical conductivities were measured on polymer films by four-point probe technique using an electrometer. Thermal data of monomer/polymer and polymers were obtained by TG-DTA and DSC techniques, respectively. © 2011 Wiley Periodicals, Inc. J Appl Polym Sci 125: 608–619, 2012

Key words: polyazomethine; cyclic voltammetry; thermal analysis; band gap; electron-donating group

INTRODUCTION

Polyazomethines (PAMs) or polymeric Schiff bases have a huge importance due to having carbon-nitrogen double bonded (—N=CH) units in the main chain capable of protonation and complexation.[1,2] In addition, aromatic PAMs have been studied intensively because of their good thermal stability, excellent mechanical strength as well as their semiconductivity and optoelectronic properties, nonlinear optical properties, ability to form metal chelates, semiconducting properties, environmental stability, fiber-forming properties.[3–10] Schiff base-substituted oligophenols and polyphenols have been studied by Kaya et al. for the last decade. This class of the polymers was mainly found to be electroactive as well as semiconductive materials and their conductivities were increased by doping with iodine.[11–15] In addition, it is known that oligophenols and their azomethine derivatives are synthesized by oxidative polycondensation (OP) reactions. OP reaction has several useful properties such as use of water as a medium, to be easy to apply, environmentally harmless, and using cheap oxidants such as NaOCl, H_2O_2, and air.[16–19] Additionally, oligophenols and their derivatives have been used in various fields, because they have useful properties such as paramagnetism, semiconductivity, electrochemical cell, and resistance to high energy. Because of these properties, they were used to prepare composites with resistance to high temperature, thermostabilizations and graphite materials, epoxy oligomer and block copolymers, adhesives, photoresists, and antistatic materials.[20–23]

To the best of our knowledge, there is no report to investigate the effect of the substituent (—CH_3) as electron-donating group on thermal stability, optical, electrochemical properties, and conductivity measurement including 4-fluorobenzaldeyhde and aromatic aminophenols (APs). For this reason, we first synthesized Schiff base monomers by condensation reaction of 4-fluorobenzaldehyde (FBA) with aromatic APs [2-AP and 2-amino-4-methylphenol (AMP)]. Then, the synthesized monomers were converted to their polyphenol derivatives via OP reaction using NaOCl as oxidant. Second, we characterized the synthesized compounds using FTIR, UV–vis spectra, ^{1}H-NMR, ^{13}C-NMR, and size exclusion chromatography (SEC) analyses. In addition, electrical, electrochemical, optical, fluorescence, and thermal

Correspondence to: İ Kaya (kayaismet@hotmail.com).

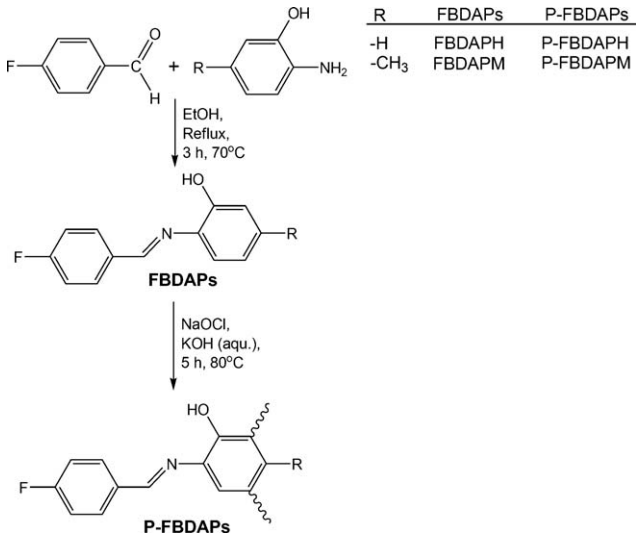

Scheme 1 Syntheses of the FBDAPs and P-FBDAPs.

properties of the synthesized polymers were investigated and the effect of the substituent (—CH_3) as electron-donating group was discussed. TG-DTA technique was used to determine the stabilities of thermal degradation. DSC analyses of the polyphenols were also carried out to determine the glass transition temperatures (T_g). Optical properties were determined by using UV–vis spectra, and the optical band gaps were calculated from absorption edges. The HOMO–LUMO energy levels and electrochemical band gap values of the compounds were obtained by using cyclic voltammetry (CV) measurements. Additionally, electrical properties of doped and undoped polymers were determined. The fluorescence spectra of the synthesized compounds were also carried out to determine maximal emission-excitation intensities. Obtained polymers were found to be semiconductive materials whose conductivities could be increased by iodine doping and the conductivity of P-FBDAPM highly increased with doping that made the polymer good candidate for gas sensing applications against electroacceptor gases such as iodine. Optical and electrochemical band gap measurements showed that the novel polymers have lower band gaps than their Schiff base monomers due to their polyconjugated structures.

EXPERIMENTAL

Materials

FBA, 2-AP, AMP, dimethylformamide (DMF), dimethylsulfoxide (DMSO), tetrahydrofuran (THF), methanol, ethanol, acetonitrile, acetone, toluene, ethyl acetate, heptane, hexane, CCl_4, $CHCl_3$, H_2SO_4, KOH, and HCl were supplied by Merck Chemical (Germany), and they were used as received. Thirty percentage aqueous solution of sodium hypo chloride, NaOCl, was supplied by Paksoy Chemical (Turkey).

Syntheses of the FBDAPs

Obtained the FBDAPs (FBDAPH and FBDAPM) were synthesized by the condensation reaction of FBA with APs (2-AP and AMP). Reactions were performed as follows: 4-fluorobenzaldeyde (2.500 g, 2×10^{-2} mol) was placed into a 250 mL three-necked round-bottom flask, which was fitted with condenser, thermometer, and magnetic stirrer. A total of 50 mL ethanol was added into the flask, and reaction mixture was heated to 60°C. A solution of equivalent amount of 2-AP (2.198 g, 2×10^{-2} mol) or AMP (2.463 g, 2×10^{-2} mol) in 20 mL ethanol was added into the flask. Reactions were maintained for 3 h under reflux. The precipitated monomers was filtered, recrystallized from acetonitrile, and dried in a vacuum desiccator. (yields: 86 and 87% for FBDAPH and FBDAPM, respectively).[13] Calcd. (%) for FBDAPH: C, 72.55; H, 4.68; N, 6.51. Found C, 72.48; H, 4.56; N, 6.45. Calcd. (%) for FBDAPM: C, 73.35: H, 5.28: N, 6.11. Found C, 73.28: H, 5.20: N, 6.00. ^{1}H-NMR (DMSO-d_6): δ ppm 9.05 (s, 1H, —OH), 8.73 (s, 1H, —CH=N), 8.12 (m, 1H, Ar-Hg) 7.36 (m, 1H, Ar-Hh), 7.23 (d, 1H, Ar-Hc), 7.10 (m, 1H, Ar-Ha), 6.93 (d, 1H, Ar-Hb), 6.85 (m, 1H, Ar-Hd) for FBDAPH and 8.92 (s, 1H, —OH), 8.73 (s, 1H, —CH=N), 8.12 (m, 1H, Ar-Hf), 7.35 (t, 1H, Ar-Hg), 7.17 (d, 1H, Ar-Ha), 6.74 (s, 1H, Ar-Hc), 6.67 (d, 1H, Ar-Hb), 2.28 (s, 3H, Ar-CH_3) for FBDAPM. ^{13}C-NMR (DMSO): δ ppm 165.01 (C12-ipso), 162.54 (C8-ipso), 151.35 (C6-ipso), 137.21 (C3-ipso), 134.75 (C7-ipso), 133.20 (C9), 131.08 (C10), 120.12 (C1), 118.49 (C2), 116.54 (C5), 115.56 (C11), 20.83 (C4) for FBDAPM.

Syntheses of the P-FBDAPs

The synthesized FBDAPs were converted to their polyphenol derivatives via OP reactions in an aqueous alkaline medium using NaOCl (30%, solution in water), as in the literature.[24] FBDAPH (0.860 g, 4×10^{-3} mol) and FBDAPM (0.916 g, 4×10^{-3} mol) were dissolved in an aqueous KOH solution (30%, 0.03 mol, 0.56 mL) and placed into a 50-mL three-necked round-bottom flask, which was fitted with a condenser, a thermometer, a stirrer, and an addition funnel containing NaOCl. After heating the solution to 40°C, NaOCl were added drop by drop within about 20 min. Then, the reaction mixtures were heated to 80°C, and reaction was maintained for 5 h. The reaction mixtures were cooled to room temperature and then they neutralized with 0.03 mol HCl solution. For the separation of mineral salts, the mixture was filtered and washed in 25 mL of hot water for three times. Then, unreacted FBDAPs were separated from the reaction products by

TABLE I
Solubility Tests of the Synthesized Compounds

Compounds	MeOH	EtOH	Ethyl acetate	$CHCl_3$	CCl_4	Acetonitrile	Toluene	Hexane	Acetone	THF	DMF	DMSO
P-FBDAPH	⊥	⊥	⊥	–	–	–	–	–	⊥	+	+	+
P-FBDAPM	–	–	–	⊥	⊥	–	–	–	⊥	+	+	+

+, soluble; –, insoluble; ⊥, partly soluble.

washing with ethanol and dried in a vacuum oven at 60°C (yields: 58 and 54% for P-FBDAPH and P-FBDAPM, respectively). All the synthesized procedures were summarized in Scheme 1.

Calcd. (%) for P-FBDAPH: C, 73.00; H, 4.08; N, 6.55. Found C, 72.85; H, 3.85; N, 6.40. Calcd. (%) for P-FBDAPM: C, 73.78; H, 4.72; N, 6.15. Found C, 73.65; H, 4.60: N, 5.95. ^{1}H-NMR (DMSO-d_6): δ ppm 9.81 (s, 1H, —OH), 8.72 (s, 1H, —CH=N), 7.89 (d, 1H, Ar-He), 7.47 (d, 1H, Ar-Hf), 6.68 (s, 1H, Ar-Hb), 6.39 (s, 1H, Ar-Ha) for FBDAPH, 8.93 (s, 1H, —OH), 8.73 (s, 1H, —CH=N), 8.11 (m, 1H, Ar-Hd), 7.35 (m, 1H, Ar-HeH), 7.17 (d, 1H, Ar-Ha), 2.26 (s, 3H, Ar-CH_3) for FBDAPM. ^{13}C-NMR (DMSO): δ ppm 165.01 (C12-ipso), 162.54 (C8-ipso), 151.35 (C6-ipso), 137.22 (C7-ipso), 134.73 (C2), 133.22 (C3-ipso), 131.08 (C9), 120.13 (C10), 118.48 (C5), 116.53 (C1), 115.77 (C11), 20.83 (C4) for FBDAPM.

Characterization techniques

The solubility tests were carried out in different solvents by using 1 mg sample and 1 mL solvent at 25°C. The infrared and ultraviolet–visible (UV–vis) spectra were measured by Perkin Elmer FTIR Spectrum one and Perkin Elmer Lambda 25, respectively. The FTIR spectra were recorded using universal ATR sampling accessory (4000–550 cm^{-1}). Elemental analyses were carried out with a LECO CHNS 932. ^{1}H- and ^{13}C-NMR spectra (Bruker AC FT-NMR spectrometer operating at 400 and 100.6 MHz, respectively) were also recorded by using deuterated DMSO-d_6 as a solvent at 25°C. The tetramethylsilane was used as internal standard. Thermal data were obtained by using Perkin Elmer Diamond Thermal Analysis. The TG-DTA measurements were made between 20 and 1000°C (in N_2, rate 10°C/min). DSC analyses were carried out by using Perkin Elmer Pyris Sapphire DSC. DSC measurements were made between 25 and 420°C (in N_2, rate 20°C/min). The number average molecular weight (M_n), weight average molecular weight (M_w), and polydispersity index (PDI) were determined by SEC techniques of Shimadzu. For SEC investigations, an SGX (100 Å and 7 nm diameter loading material) 3.3 mm i.d. × 300 mm columns was used; eluent: DMF (0.4 mL/min), polystyrene standards were used. Moreover, refractive index detector a UV detector was used to analyze the products at 25°C.

Optical and electrochemical properties

The optical band gaps (E_g) of the synthesized compounds were calculated from their absorption edges. UV–vis spectra were measured by Perkin Elmer Lambda 25. The absorption spectra were recorded by using DMSO at 25°C.

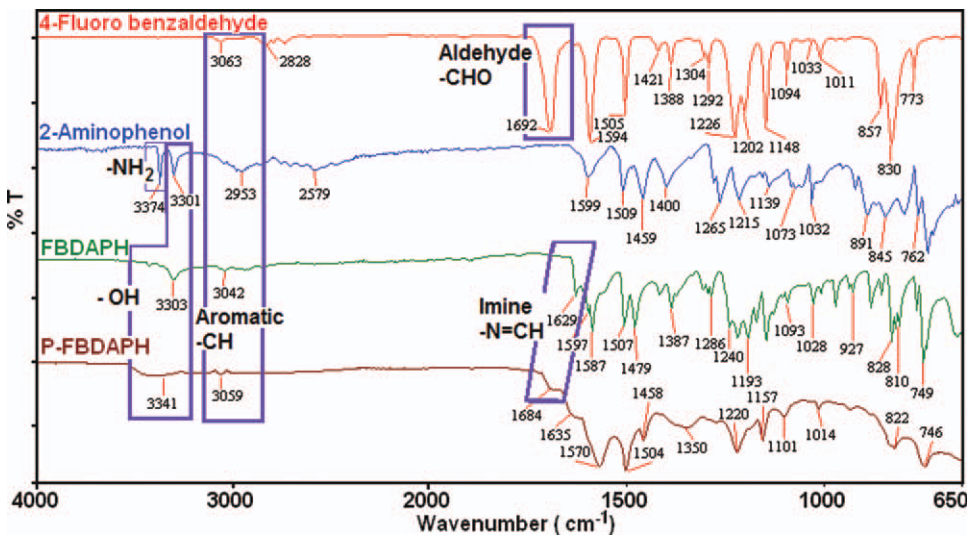

Figure 1 FTIR spectra of FBA, AP, FBDAPH and P-FBDAPH. [Color figure can be viewed in the online issue, which is available at wileyonlinelibrary.com.]

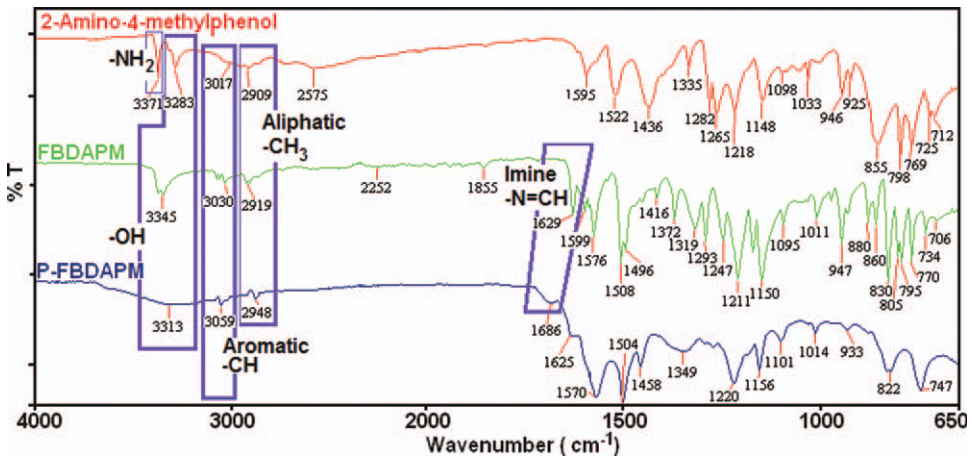

Figure 2 FTIR spectra of AMP, FBDAPM and P-FBDAPM. [Color figure can be viewed in the online issue, which is available at wileyonlinelibrary.com.]

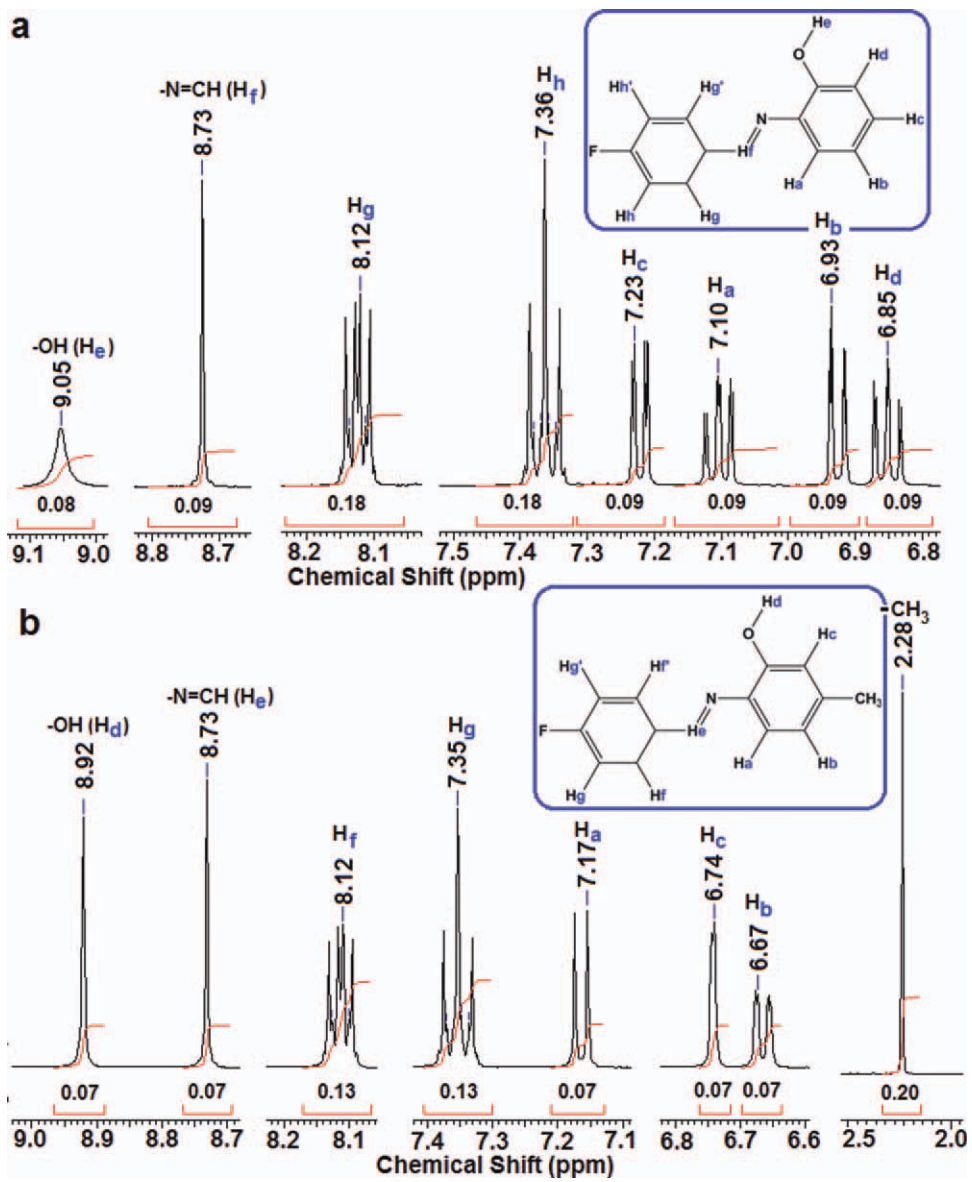

Figure 3 ^{1}H-NMR spectra of FBDAPH (a) and FBDAPM (b). [Color figure can be viewed in the online issue, which is available at wileyonlinelibrary.com.]

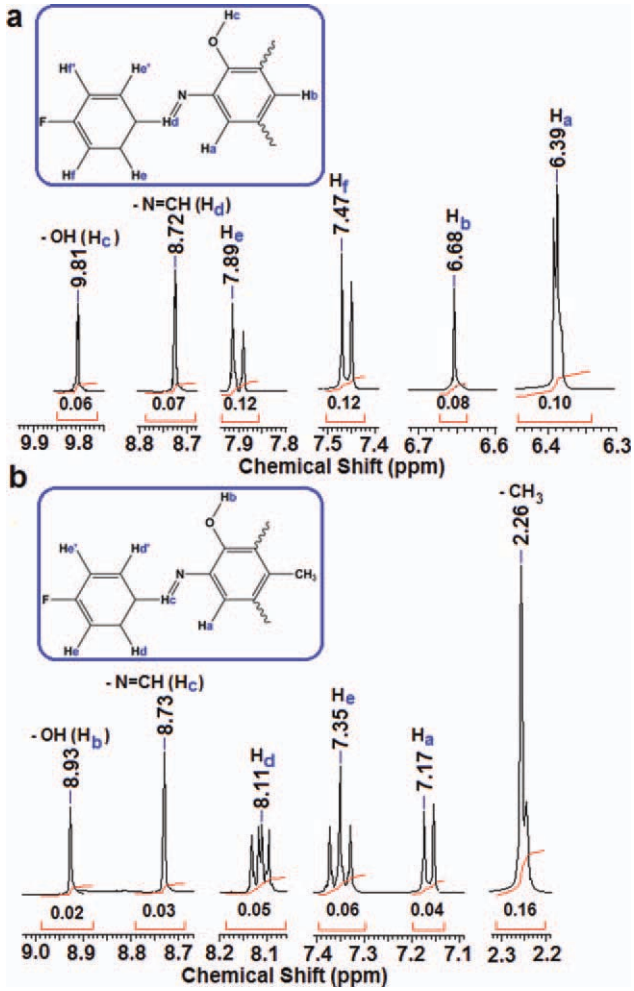

Figure 4 ^{1}H-NMR spectra of P-FBDAPH (a) and P-FBDAPM (b). [Color figure can be viewed in the online issue, which is available at wileyonlinelibrary.com.]

CV measurements were carried out with a CHI 660C Electrochemical Analyzer (CH Instruments, TX) at a potential scan rate of 20 mV/s. All the experiments were performed in a dry box filled with argon at room temperature. The electrochemical potential of Ag was calibrated with respect to the ferrocene/ferrocenium (Fc/Fc^+) couple. The half-wave potential ($E^{1/2}$) of (Fc/Fc^+) measured in 0.1*M* tetrabutylammonium hexafluorophosphate acetonitrile solution is 0.39 V with respect to Ag wire. The voltammetric measurements were carried out in acetonitrile and DMSO.[11] An ultrasonic bath was used to solve the samples. The HOMO–LUMO energy levels and electrochemical band gaps (E'_g) were calculated from the oxidation and reduction onset values.

Electrical properties

Conductivities of the synthesized materials were measured on a Keithley 2400 Electrometer. The pellets were pressed on a hydraulic press developing up to 1687.2 kg/cm^2. Iodine doping was carried out by exposure of the pellets to iodine vapor at atmospheric pressure and room temperature in a desiccator.[25]

Fluorescence measurements

A Shimadzu RF-5301PC spectrofluorophotometer was used in fluorescence measurements. Emission and excitation spectra of the synthesized compounds were obtained in solution forms in DMF, THF, and DMSO for both the monomers and the polymers. Measurements were made in a wide concentration range between 0.15 and 19.20 mg/L to determine the optimal fluorescence concentrations. Slit width in all measurements was 3 nm. Fluorescence quantum yields were determined by comparative method as described by Williams et al.[26]

RESULTS AND DISCUSSION

Solubilities and structures of the compounds

The synthesized monomers have light color-powder forms, whereas their polyphenol derivatives are dark colored. The solubility test results are shown in Table I. The synthesized Schiff bases are completely soluble in used all of solvent except *n*-hexane. According to Table I, the synthesized PAMUs are completely soluble in highly polar solvents such as THF, DMF, and DMSO, and partly soluble in acetone, whereas insoluble in acetonitrile, toluene, *n*-hexane. P-FBDAPH is partly soluble in MeOH, EtOH, and ethyl acetate, whereas insoluble in $CHCl_3$ and CCl_4. P-FBDAPM is partly soluble in $CHCl_3$ and CCl_4, whereas insoluble in MeOH, EtOH, and ethyl acetate. As a result, the synthesized monomers (FBDAPH and FBDAPM) have higher solubilities compared with their polyphenol derivatives (P-FBDAPH and P-FBDAPM), because P-FBDAPH and P-FBDAPM have higher molecular weights than the synthesized monomers.

FTIR spectral data of 4-fluoro benzaldehyde, 2-AP, FBDAPH, and P-FBDAPH are given Figure 1. Similarly, AMP, FBDAPM, and P-FBDAPM are given Figure 2. As seen in Figures 1 and 2, the structures of the synthesized monomers are confirmed by growing imine (—CH=N) peaks with disappearing of the —NH_2 peak of APs and the —CHO peak of the FBA used in the condensation reactions. According to Figure 1 at the spectrum of 4-fluoro benzaldehyde characteristic aldehyde (—CHO) peak is observed at 1692 cm^{-1} and 2-AP and 2-methyl-4-aminophneol —NH_2 peaks are observed at 3374 and 3371 cm^{-1}, respectively. At the spectra of FBDAPH and FBDAPM imine (—CH=N) peak is observed at 1629 and 1629 cm^{-1}, respectively. At the spectra of

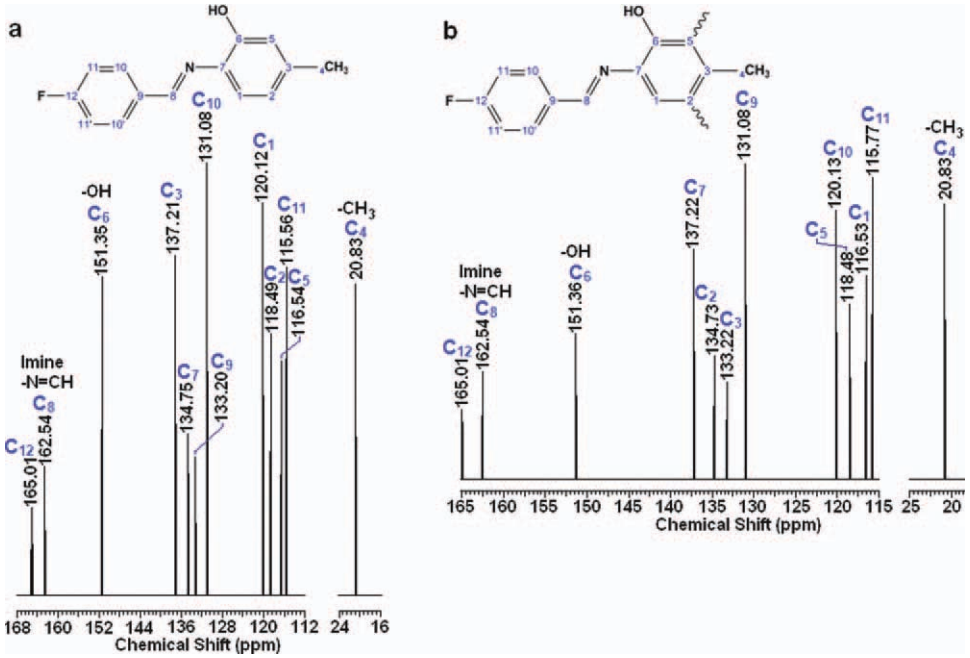

Figure 5 ^{13}C-NMR spectra of FBDAPM (a) and P-FBDAPM (b). [Color figure can be viewed in the online issue, which is available at wileyonlinelibrary.com.]

P-FBDAPH and P-FBDAPM the same peak is observed at 1684 and 1686 cm^{-1}, respectively. In addition, —OH stretch of phenolic groups is observed in the range of at 3301–3345 cm^{-1}. At the spectra of polymers, the peaks also broaden due to the polyconjugated structures.

^{1}H-NMR spectra of FBDAPH and FBDAPM are given in Figure 3. In addition, the same spectra of P-FBDAPH and P-FBDAPM are given in Figure 4. Similarly, ^{13}C-NMR spectra of FBDAPM and P-FBDAPM are given in Figures 5(a,b), respectively. According to Figure 3(a) at the spectrum of FBDAPH —OH and imine (—CH=N), peaks are observed at 9.05 and 8.73 ppm, respectively. At the spectrum of FBDAPM, the same peaks are observed at 8.92 and 8.73 ppm, respectively. At the spectra of P-FBDAPH and P-FBDAPM, these peaks are observed at 9.81 and 8.93 ppm and 8.72 and 8.73 ppm, respectively. Additionally, methyl (—CH_3) substituent of FBDAPM and P-FBDAPM is observed 2.26 ppm. According to the ^{1}H-NMR results, after the polymerization, the peak values of the —OH protons shifted to higher chemical shifts.

^{13}C-NMR spectrum of FBDAPM at Figure 5(a) also confirms the structure by the peaks observed at 162.54 and 151.35 ppm, which could be attributed to the imine (—CH=N) and —OH carbons, respectively. At the spectrum of P-FBDAPM at Figure 5(b), these peaks are observed at 162.54 and 151.36 ppm, respectively. Additionally, aliphatic —CH_3 peak is observed at 20.83 ppm both FBDAPM and P-FBDAPM. These results clearly show that the synthesized polymers are obtained with the proposed structures shown in Scheme 1.

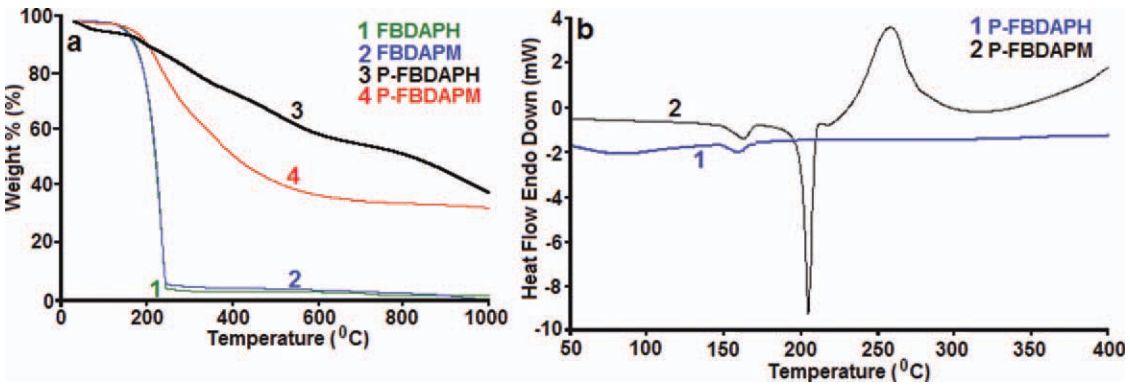

Figure 6 TGA curves of the synthesized compounds (a) and DSC curves of P-FBDAPH and P-FBDAPM (b). [Color figure can be viewed in the online issue, which is available at wileyonlinelibrary.com.]

TABLE II
Thermal Degradation Values of the Synthesized Compounds

Compounds	T_{on}[a]	$W_{max.}T$[b]	20% weight losses	50% weight losses	Char at 1000°C (%)	DSC	
						T_g[c] (°C)	ΔC_p[d] (J/g°C)
FBDAPH	184	227	197	216	1.60	–	–
FBDAPM	189	225	195	221	0.25	–	–
P-FBDAPH	167	194,301,508	375	849	42.66	154	0.019
P-FBDAPM	173	229,365	246	407	33.08	156	0.564

[a] The onset temperature.
[b] Maximum Weight Temperature.
[c] Glass Transition Temperature.
[d] Change of specific heat during glass transition.

Thermal analyses

TG-DTA and DSC curves of the synthesized compounds are given in Figure 6. The results of TG-DTA and DSC are also summarized in Table II. According to the TGA results, the onset temperatures of the polymers are generally lower than those of their monomers. TGA results show that the synthesized polymers lost 50% of their weights at 849 and 407°C and their char residues at 1000°C are 42.66 and 33.08% for P-FBDAPH and P-FBDAPM, respectively. This result show that P-FBDAPH derived from 2-AP has higher the char residues than P-FBDAPM derived from AMP. On the other hand, P-FBDAPM has a bit higher onset temperatures than P-FBDAPH. According to the DSC traces, the glass transition temperatures (T_g) of P-FBDAPH and P-FBDAPM are 154 and 156°C, respectively, and these results show that there are not significant different between the glass transition temperatures of P-FBDAPH and P-FBDAPM. The broad peaks until 135°C could be attributed to the absorbed solvent removal.

Size exclusion chromatography

According to the SEC chromatograms, the calculated number–average molecular weight (M_n), weight average molecular weight (M_w), and PDI values of P-FBDAPH and P-FBDAPM measured using UV detector. The M_n, M_w, and PDI values of and were found as 38,000, 48,100, 1.266 for P-FBDAPH and 22,900, 30,250, 1.320 for P-FBDAPM, respectively. According to these results, P-FBDAPH and P-FBDAPM contain approximately 223–224 and 100–131 repeated units, respectively. The obtained results confirm the polymer structures. According to these results, the synthesized polymers have quite high molecular weights. However, as emphasized in a previous study, molecular weight of a OP product could be affected by reaction conditions used.[27] As a result, the obtained molecular weight could be varied by changing of the polycondensation conditions.

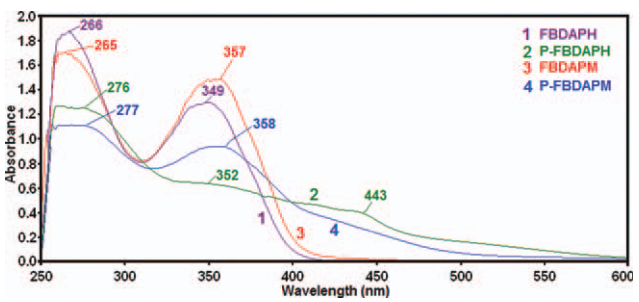

Figure 7 UV-vis spectra of FBDAPH, P-FBDAPH, FBDAPM, and P-FBDAPM. [Color figure can be viewed in the online issue, which is available at wileyonlinelibrary.com.]

Optical and electrochemical properties

The UV–vis spectra of the synthesized compounds were shown in Figure 7. According to Figure 7, π–π* transition peaks of the synthesized compounds are appeared around 350–360 due to azomethine linkage (—CH=N) in the structure. In addition, the absorption edges of the synthesized polymers shifted to higher wave length values because of the polyconjugated structures of the polymers which increase HOMO and decrease LUMO energy levels thus resulting in lower band gaps. The optical band gaps (E_g) were calculated as in the literature[28] and are given in Table III.

The cyclic voltammograms of the synthesized compounds are shown in Figure 8. According to the

TABLE III
Electronical Structure Parameters of the Synthesized Compounds

Compounds	HOMO[a] (eV)	LUMO[b] (eV)	E_g[c] (eV)	E'_g[d] (eV)
FBDAPH	−5.99	−2.60	3.10	3.39
FBDAPM	−5.76	−2.79	2.65	2.97
P-FBDAPH	−5.88	−2.68	3.07	3.20
P-FBDAPM	−5.83	−2.99	3.04	2.84

[a] Highest occupied molecular orbital.
[b] Lowest unoccupied molecular orbital.
[c] Optical band gap.
[d] Electrochemical band gap.

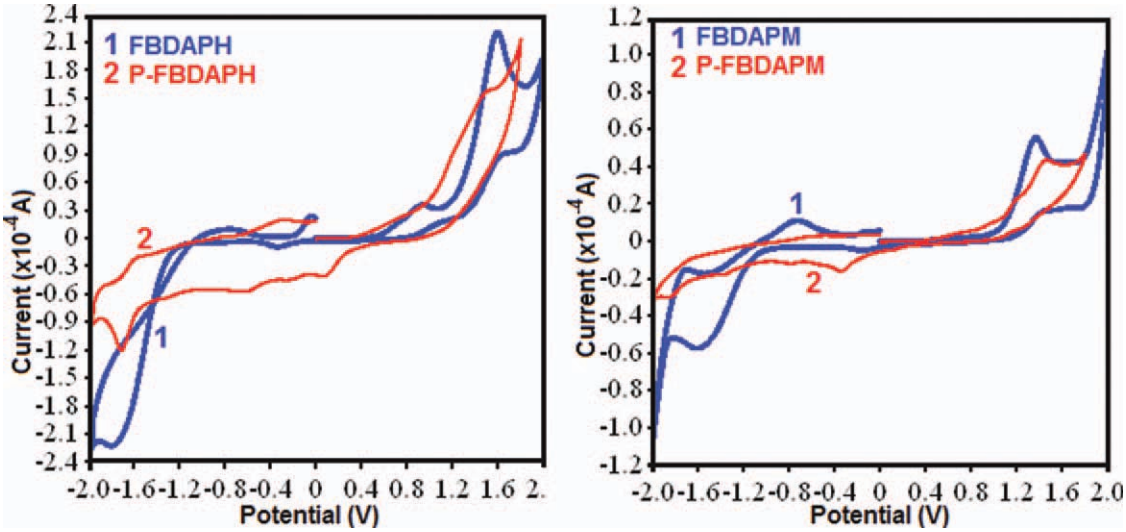

Figure 8 Cyclic voltammograms of FBDAPH, P-FBDAPH, FBDAPM, and P-FBDAPM. [Color figure can be viewed in the online issue, which is available at wileyonlinelibrary.com.]

CV measurements, the calculated HOMO–LUMO energy levels and the electrochemical band gaps (E'_g) were shown in Table III. These data were estimated by using the oxidation onset (E_{ox}) and reduction onset (E_{red}) values. The calculations were made by using the following equations[29]:

$$E_{HOMO} = -(4.39 + E_{ox}) \quad (1)$$

$$E_{LUMO} = -(4.39 + E_{red}) \quad (2)$$

$$E'_g = E_{LUMO} - E_{HOMO} \quad (3)$$

The HOMO–LUMO energy levels and the electrochemical band gaps were also shown schematically in Figure 9. As shown in Figure 9, the order of electrochemical band gaps is as follows: FBDAPH > P-FBDAPH > FBDAPM > P-FBDAPM. Obtained results indicate that after the polycondensation reactions, HOMO energy levels increase while LUMO energy levels decrease, and so, the electrochemical band gaps (E'_g) of the polymers are lower than those of the monomers. Lower band gaps facilitate the electronic transitions between HOMO–LUMO energy levels and make the polymers more electroconductive than the monomers. According to the electrochemical analysis results, P-FBDAPH has higher electrochemical band gap (E'_g) than P-FBDAPM. Similarly, FBDAPH has higher electrochemical band gap (E'_g) than FBDAPM. This can be probably due to electron density of the synthesized compounds. FBDAPM and P-FBDAPM have methyl group (—CH_3) para position of carbon atom which is simultaneously bound with the imine nitrogen while FBDAPH and P-FBDAPH have hydrogen atom para position of the same carbon. In addition, —CH_3 group is an electron-donating group and it partly increases the electron density of ortho and para positions of the aromatic ring.[7]

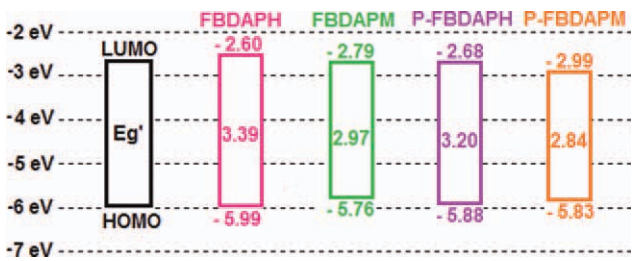

Figure 9 HOMO–LUMO energy levels and electrochemical band gaps of the synthesized compounds. [Color figure can be viewed in the online issue, which is available at wileyonlinelibrary.com.]

Electrical conductivities

Electrical conductivities of the synthesized polyphenol and the changes of these values related to doping time with iodine are determined and summarized in Table IV. The changes of the electrical

TABLE IV
Electrical Conductivity Results of I_2-Doped and -Undoped Compounds versus Doping Time at 25°C

	Conductivity (S cm^{-1}) × 10^{-10}	
Time (h)	P-FBDAPH	P-FBDAPM
0	1.48	1.08
24	75.18	114.94
48	285.71	1428.57
72	751.08	3456.10
96	1347.71	11415.50
120	3154.57	28011.20
144	6896.55	97087.40
168	15674.00	163934.00

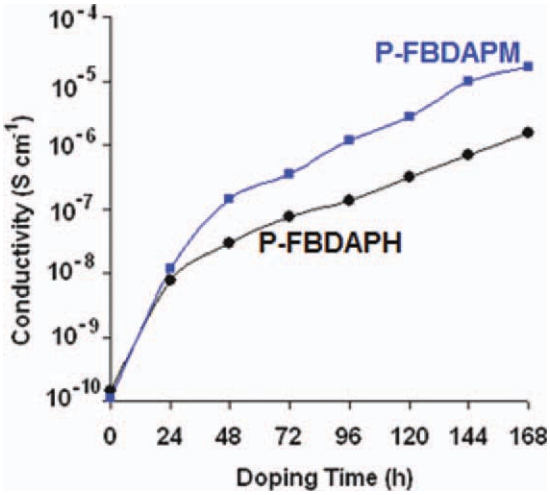

Figure 10 Changes of the electrical conductivities of the I_2-doped and undoped compounds vs. doping time at 25°C. [Color figure can be viewed in the online issue, which is available at wileyonlinelibrary.com.]

conductivities are also given schematically in Figure 10. As seen in Figure 10 and Table IV, P-FBDAPH has higher electrical conductivity than P-FBDAPM at the undoped state but P-FBDAPM has higher electrical conductivity than P-FBDAPH at the doped state. However, after a long time iodine doping for 168 h the conductivities nearly increased 10590 and 151790 times of their magnitudes for P-FBDAPH and P-FBDAPM. According to these results, P-FBDAPH has $\sim$ 1.50 times higher undoped conductivity (1.48×10^{-10}) than P-FBDAPM. On the other hand, the synthesized polymers when doped with iodine for 168 h P-FBDAPM has $\sim$ 10.50 times higher than P-FBDAPH. Doping mechanism of imine polymers has been previously studied and presented in the literature.[23] According to the proposed mechanism, nitrogen is capable of coordinating with an iodine molecule due to it being a very electronegative element. Consequently, a charge-transfer complex between imine compound and dopant iodine is formed and a considerable increase in conductivity can be observed. The synthesized P-FBDAPM has methyl (—CH_3) substituent on the structure takes part of para position of carbon atom, which is simultaneously bound with the imine nitrogen. As known —CH_3 substituent as an electron-donating group partly increases the electron density of ortho and para positions of the aromatic ring. As a result, the electron density on carbon atom, which is simultaneously bound with the imine nitrogen of P-FBDAPM becomes higher than P-FBDAPH. This also increases the electron density on the imine nitrogen and consequently ability of iodine doping. Total charges of imine nitrogens are also calculated by Huckel Calculation method[7] and given in Figure 11. As a result of the calculation the charge of imine nitrogen is -0.449 for P-FBDAPM while -0.217 for P-FBDAPH. These results support the obtained conductivity increases as mentioned above; with higher electron density P-FBDAPM could be highly doped when exposure to iodine vapor. Consequently, the conductivity of P-FBDAPM could be highly increased and used as the semiconductive polymer in electronic, optoelectronic, and photovoltaic applications such as photovoltaic solar cell, solar panels, and photovoltaic inspection system.

Fluorescence characteristics

Fluorescence measurements of the synthesized compounds are carried out using different solvent such as THF, DMF, and DMSO for the monomers and their polyphenol derivatives. Measurements are made for various concentrations to determine the optimal conditions. Figure 12 show the excitation and emission spectra of FBDAPH, FBDAPM, P-FBDAPH, and FBDAPM in different solvents. Figure 13 also indicate the concentration-fluorescence intensity relationships of the compounds. The obtained results are also summarized in Table V. According to Table V, the optimum concentration to obtain maximal emission–excitation intensities change between 9.60–0.30 mg/L. These results clearly indicate that FBDAPH has higher fluorescence intensity than FBDAPM. Similarly, P-FBDAPH has higher

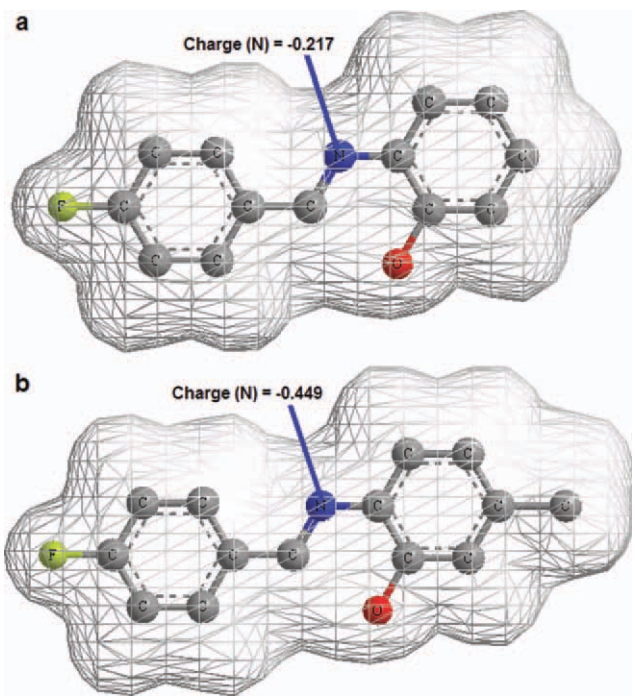

Figure 11 Total charge density distribution views of FBDAPH (a) and FBDAPM (b) (H atoms are not shown). [Color figure can be viewed in the online issue, which is available at wileyonlinelibrary.com.]

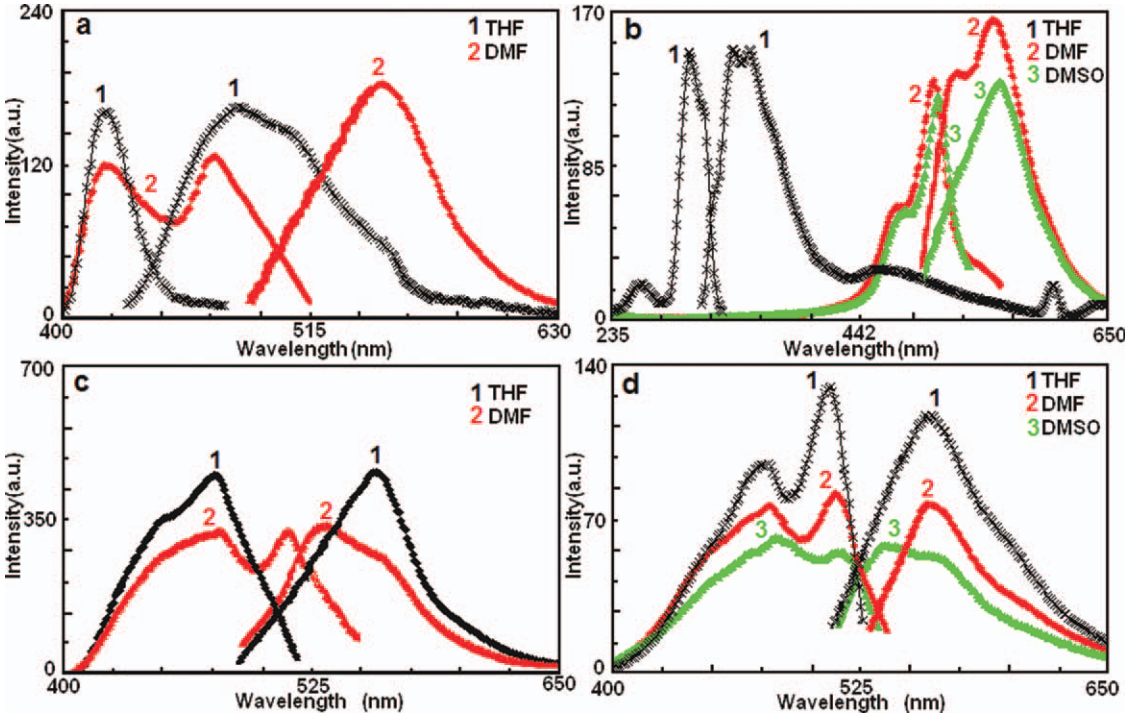

Figure 12 Emission and excitation spectra of FBDAPH (a), P-FBDAPH (b), FBDAPM (c) and P-FBDAPM (d) in various solvent. Slit width: λ_{Ex}: 3 nm, λ_{Em}: 3 nm. [Color figure can be viewed in the online issue, which is available at wileyonlinelibrary.com.]

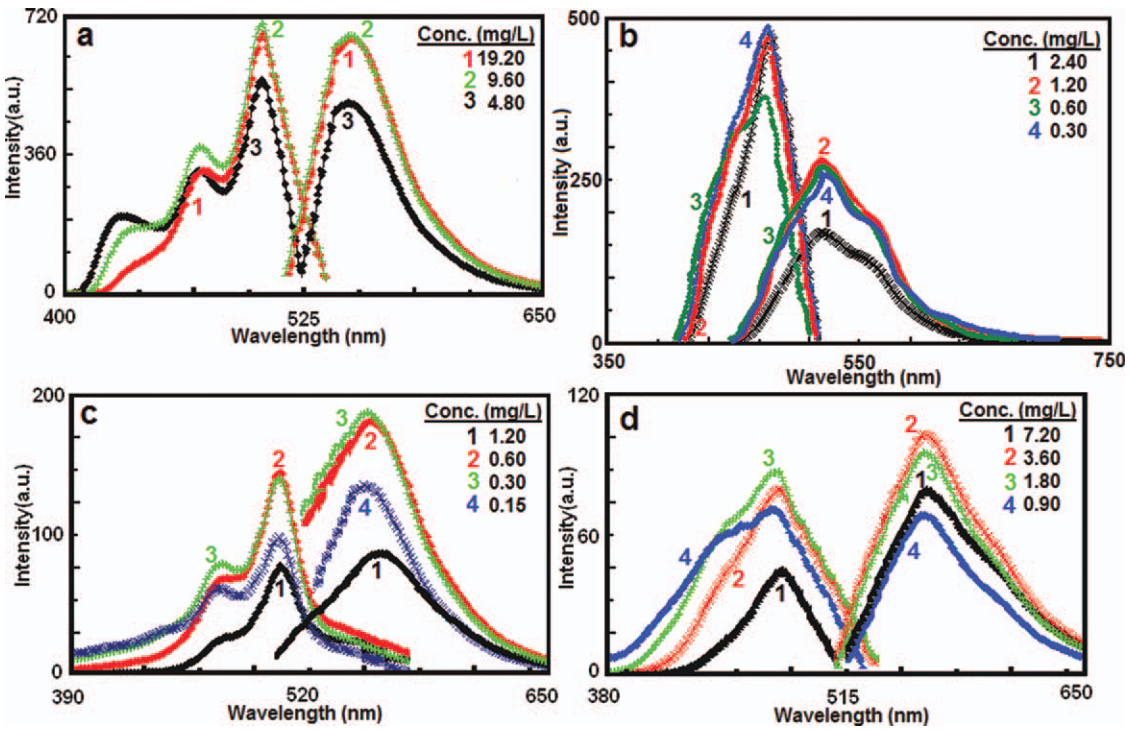

Figure 13 Emission and excitation spectra of various concentrated solutions of FBDAPH (a), FBDAPM (b), P-FBDAPH (c) and P-FBDAPM (d) in THF (a, c, d) and DMF (b). Slit width: λ_{Ex}: 3 nm, λ_{Em}: 3 nm. [Color figure can be viewed in the online issue, which is available at wileyonlinelibrary.com.]

TABLE V
Fluorescence Spectral Data of the Synthesized Compounds

Compounds	Conc. (mg/L)	λ_{Ex}[a]	λ_{Em}[b]	$\lambda_{max\ (Ex)}$[c]	$\lambda_{max\ (Em)}$[d]	I_{Ex}[e]	I_{Em}[f]	Q.Y.[g] (%)
FBDAPH	9.60	503	518	503	520	698	710	–
FBDAPM	1.20	441	521	477	519	470	285	–
P-FBDAPH	0.30	505	571	503	550	140	188	0.95
P-FBDAPM	3.60	511	527	510	557	107	102	0.2

[a] Excitation wavelength for emission.
[b] Emission wavelength for excitation.
[c] Maximum emission wavelength.
[d] Maximum excitation wavelength.
[e] Maximum excitation intensity.
[f] Maximum emission intensity.
[g] Photo luminescence quantum yield.

fluorescence intensity than P-FBDAPM. P-FBDAPH and P-FBDAPM give the emission peaks at 550 and 557 nm with the intensities of 188 and 102 nm, respectively. Fluorescence characteristics of P-FBDAPH and P-FBDAPM resembles those of "Acridine Yellow," and "Alexa Fluor 532" presented in the literature.[30] Acridine yellow and Alexa Fluor 532 have emission peaks at 550 and 557 nm and excitation peaks at 470 and 530 nm, respectively. Similarly, the new presented P- FBDAPH and P-FBDAPM have the 503 and 510 nm excitation and 550 and 557 nm emission peaks, respectively. Photoluminescence (PL) quantum yield of the polymer is measured as described elsewhere[26] and found to be $\sim$ 0.95 and 0.2% for P-FBDAPH and P-FBDAPM, respectively. Relatively low quantum yield of the polymer can be explained by the formation of carbonyl function (due to over oxidation) in polymer backbone in low amount. It is well known that the carbonyl moieties are good fluorescence quenchers, because an intercrossing process is favored by their n–π^* transition.[31]

CONCLUSIONS

Novel monomers and their polyphenol derivatives of azomethine compounds including FBA and aromatic AP were synthesized by condensation and OP reaction, respectively. The synthesized materials were characterized by UV–vis, FTIR, NMR, and SEC analyses. PL spectra of the synthesized compounds were obtained using different solvent such as DMF, THF, and DMSO. The obtained results show that the synthesized compounds have highly fluorescent and can be used in preparation of the alternative yellowish emitting diodes. Electrochemical and optical properties of the synthesized compounds were also investigated and it was found that the synthesized polyphenols have quite lower band gaps than the monomers due to their polyconjugated structures. Electrical conductivity measurements show that the synthesized polymers are semiconductors and they can be used as semiconductive polymer in electronic, optoelectronic, and photovoltaic applications. The obtained results show that P-FBDAPH has higher conductivity undoped state, whereas P-FBDAPM has higher conductivity doped state due to P-FBDAPM has higher electron density than P-FBDAPH. However, TGA results showed that FBDAPM and P-FBDAPM have higher thermal stabilities as compared to FBDAPH and P-FBDAPH. DSC results showed that the new polyphenol derivatives derived from FBA with APs have T_g values 154 and 156°C. Consequently, because of the fine thermal properties the synthesized compounds can be promising candidates for aerospace applications and they can be used to produce temperature-stable materials.

References

1. Grigoras, M.; Catanescu, C. J Macromol Sci C: Polym Rev 2004, 44, 131.
2. Iwan, A.; Sek, D. Prog Polym Sci 2008, 33, 289.
3. Yıldırım, M.; Kaya, İ. Polymer 2009, 50, 5653.
4. Kaya, İ.; Çulhaoğlu, S.; Gül, M. Synth Met 2006, 156, 1123.
5. McElvain, J.; Tatsuura, S.; Wudl, F.; Heeger, A. J. Synth Met 1998, 95, 101.
6. Marin, L.; Cozan, V.; Bruma, M.; Grigoras, V. C. Eur Polym J 2006, 42, 1173.
7. Kaya, İ.; Yıldırım, M.; Avcı, A. Synth Met 2010, 160, 911.
8. Kaya, İ.; Aydın, A. E-Polymer 2008,071.
9. Wang, C. G.; Shieh, S.; LeGoff, E.; Kanatzidis, M. G. Macromolecules 1996, 29, 3147.
10. Kaya, İ.; Vilayetoğlu, A. R.; Mart, H. Polymer 2001, 42, 4859.
11. Kaya, İ.; Yıldırım, M. Eur Polym J 2007, 43, 127.
12. Kaya, İ.; Yıldırım, M. Synth Met 2009, 159, 1572.
13. Kaya, İ.; Yıldırım, M.; Kamacı, M. Eur Polym J 2009, 45, 1586.
14. Kaya, İ.; Yıldırım, M.; Aydın, A.; Şenol, D. React Funct Polym 2010, 70, 815.
15. Kaya, İ.; Şenol, D. J Appl Polym Sci 2003, 90, 442.
16. Şahmetlioğlu, E.; Arıkan, U.; Toppare, L.; Yuruk, H.; Mart, H. J Macromol Sci A, Pure Appl Chem 2006, 43, 1523.
17. Mart, H. Des Monomers Polym 2006, 9, 551.
18. Mamedov, B. A.; Vidadi, Y. A.; Alieva, D. N.; Ragimov, A. V. Polym Int 1997, 43, 126.
19. Kaya, İ.; Koça, S. Polymer 2004, 45, 1743.
20. Kaya, İ.; Yıldırım, M.; Aydın, A. Org Electron 2011, 12, 210.

21. Kaya, İ.; Kızılkaya, B.; Özdemir, E. Polym-Plast Technol Eng 2005, 44, 1307.
22. Baughman, R. H.; Bredas, J. L.; Chance, R. R.; Elsenbaumer, R. L.; Shacklette, L. W. Chem Rev 1982, 82, 209.
23. Diaz, F. R.; Moreno, J.; Tagle, L. H.; East, G. A.; Radic, D. Synth Met 1999, 100, 187.
24. Kaya, İ.; Bilici, A.; Saçak, M. Synth Met 2009, 159, 1414.
25. Kaya, İ.; Yıldırım, M. J Appl Polym Sci 2007, 106, 2282.
26. Alun, T.; Williams, R.; Winfield, S. A.; Miller, J. N. Analyst 1983, 108, 1067.
27. Akgul, C.; Yıldırım, M. J Serb Chem Soc 2010, 75, 1203.
28. Colladet, K.; Nicolas, M.; Goris, L.; Lutsen, L.; Vanderzande, D. Thin Solid Films 2004, 451, 7.
29. Cervini, R.; Li, X. C.; Spencer, G. W. C.; Holmes, A. B.; Moratti, S. C.; Friend, R. H. Synth Met 1997, 84, 359.
30. http://www.iss.com/resources/reference/data_tables/LifetimeDataFluorophores.html.
31. Ranger, M.; Rondeau, D.; Leclerc, M. Macromolecules 1997, 30, 7686.